

Fluid Simulations for Laser-Produced Plasmas

Milan Kuchařík[†]

[†] Faculty of Nuclear Sciences and Physical Engineering, Czech Technical University in Prague,
Břehová 7, Praha 1, 115 19, Czech Republic

milan.kucharik@fjfi.cvut.cz, <http://kfe.fjfi.cvut.cz/~kucharik>

D12MMVP

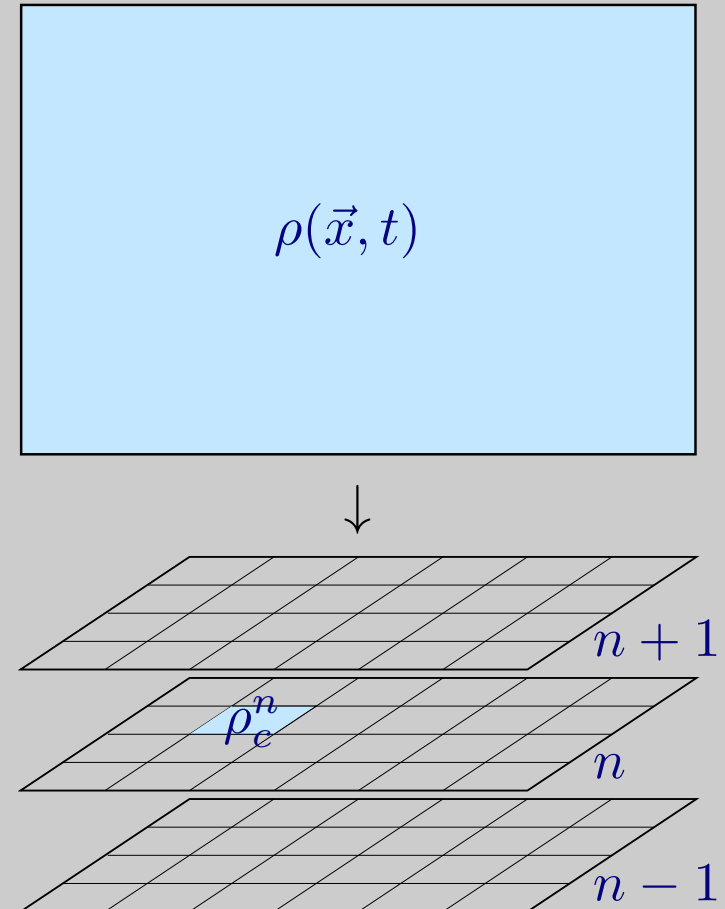
Prague, April 24, 2023

Overview

- Hydrodynamic simulations.
- Euler equations in Eulerian and Lagrangian frameworks.
- Arbitrary Lagrangian-Eulerian (ALE) methods.
- Staggered compatible Lagrangian scheme.
- Mesh rezoning techniques.
- Quantity remapping.
- Physical models for LPP.
- Examples of hydrodynamic ALE simulations.
- Conclusions.

Hydrodynamic (fluid) simulations

- Hydrodynamics = dynamics of fluids.
- Description of fluid by a set of (hyperbolic) PDEs, solution by tools of Computational Fluid Dynamics (CFD).
- Fluid properties represented by macroscopic quantities – density, velocity, pressure, specific internal energy, . . .
- Discretization:
 - space: computational mesh, cells c ;
 - time: sequence of meshes, time levels n .
- Approximation of continuous density (other quantity) function $\rho(\vec{x}, t)$ by its discrete values $\rho_c^n = \rho(\vec{x}_c, t^n)$.
- Transformation of system of PDEs for $\rho(\vec{x}, t)$ to system of algebraic equations for ρ_c^n .



Euler equations

- Simplest approximation – Euler equations.
- System of hyperbolic PDEs representing conservation of mass, momentum, and total energy:

$$\rho_t + \operatorname{div}(\rho \vec{w}) = 0, \quad (1)$$

$$(\rho \vec{w})_t + \operatorname{div}(\rho \vec{w}^2) + \overrightarrow{\operatorname{grad}} p = 0, \quad (2)$$

$$E_t + \operatorname{div}(\vec{w} (E + p)) = 0. \quad (3)$$

- Here: ρ – density, \vec{w} – velocity, p – pressure, $E = \rho \varepsilon + \frac{1}{2} \rho |\vec{w}|^2$ – total energy density, ε – specific internal energy.
- More unknowns than equations – system enclosed by equation of state (EOS): $p = \mathcal{P}(\rho, \varepsilon)$. Ideal gas – $p = (\gamma - 1) \rho \varepsilon$, where γ – gas constant (ratio of its specific heats).
- General fluid (plasma) – complicated (non-linear) EOSes, often tabulated.

Transformation from Eulerian to Lagrangian framework

- Transforming system to moving (Lagrangian) reference frame.
- Example – conservation of mass in 1D: $\rho_t + (\rho u)_x = 0$, expanding derivative:
 $\rho_t + u \rho_x + \rho u_x = 0$.
- This can be written as $\frac{D\rho}{Dt} + \rho u_x = 0$, where $\frac{D}{Dt} = \frac{\partial}{\partial t} + \frac{\partial x}{\partial t} \frac{\partial}{\partial x} = \frac{\partial}{\partial t} + u \frac{\partial}{\partial x}$ is the Lagrangian (total, material) derivative.
- In multiD: $\frac{D}{Dt} = \frac{\partial}{\partial t} + \vec{w} \cdot \nabla$.
- Similarly for the whole system:

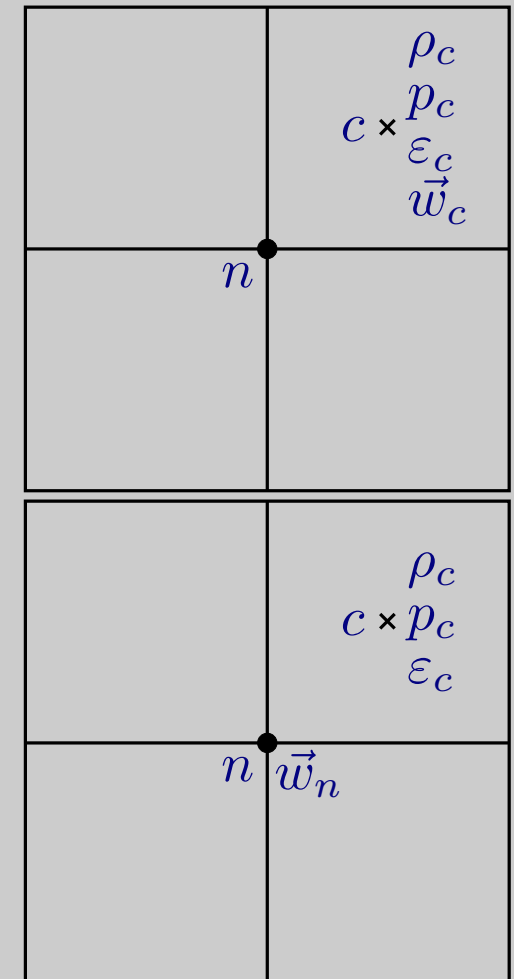
$$\frac{D\rho}{Dt} + \rho \nabla \cdot \vec{w} = 0, \quad (4)$$

$$\rho \frac{D\vec{w}}{Dt} + \nabla p = \vec{0}, \quad (5)$$

$$\rho \frac{D\varepsilon}{Dt} + p \nabla \cdot \vec{w} = 0. \quad (6)$$

Lagrangian motion

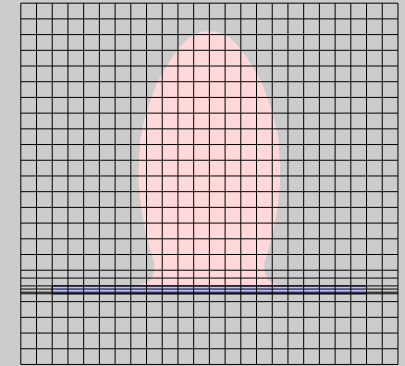
- Motion of Lagrangian particles described by an ODE: $\frac{D\vec{x}}{Dt} = \vec{w}$, typically defines motion of mesh nodes.
- Location of velocity w :
 - in mesh cells \rightarrow **cell-centered methods**: all quantities located at the same place, need to use approximate Riemann solver at each node to define its velocity;
 - in mesh nodes \rightarrow **staggered methods**: mesh motion directly defined, different location of thermodynamic ($\rho_c, p_c, \varepsilon_c$) and kinematic (\vec{w}_n) quantities.
- Computational cells considered to be Lagrangian particles: no mass flux between cells \Rightarrow density given by cell shape (volume), no need to solve mass equation.



Euler equation – notes

- Eulerian form – usually for conservative quantities, Lagrangian form – usually for primitive quantities, equivalent.
- Inter-connected system of PDEs \rightarrow cannot be solved analytically (except for few special cases) \Rightarrow numerical methods.
- Remains to define IC ($\rho(\vec{x}, t = 0) = \rho_0(\vec{x})$) and BC (wall, free, periodic, physics dependent, . . .) – can be most difficult.

Eulerian vs. Lagrangian methods

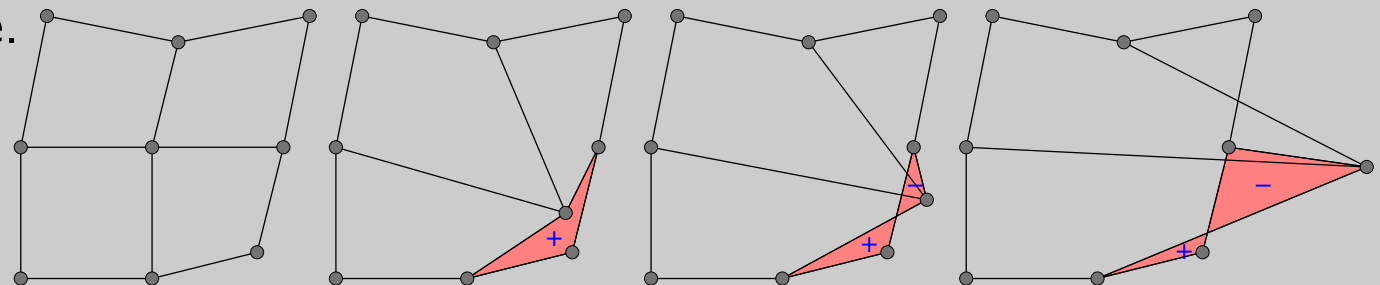
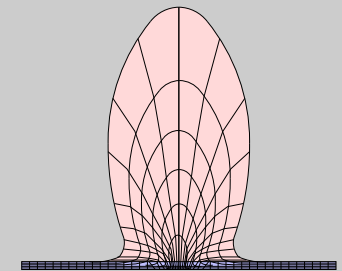


- **Eulerian methods:**

- Fixed computational mesh, not changing in time.
- Fluid moves between mesh cells in the form of mass fluxes.
- Simpler methods, easier to analyze.
- **Problem:** Not suitable for highly-volume-changing problems – typical in laser/plasma simulations, where strong material compressions and expansions occur.

- **Lagrangian methods:**

- Computational mesh moves naturally with the fluid.
- No mass fluxes, constant masses in cells.
- Optimal for strongly changing domains.
- **Problem:** Due to mesh motion, mesh can degenerate – non-convex, self-intersecting, or completely inverted cells → increase of numerical error or simulation failure.

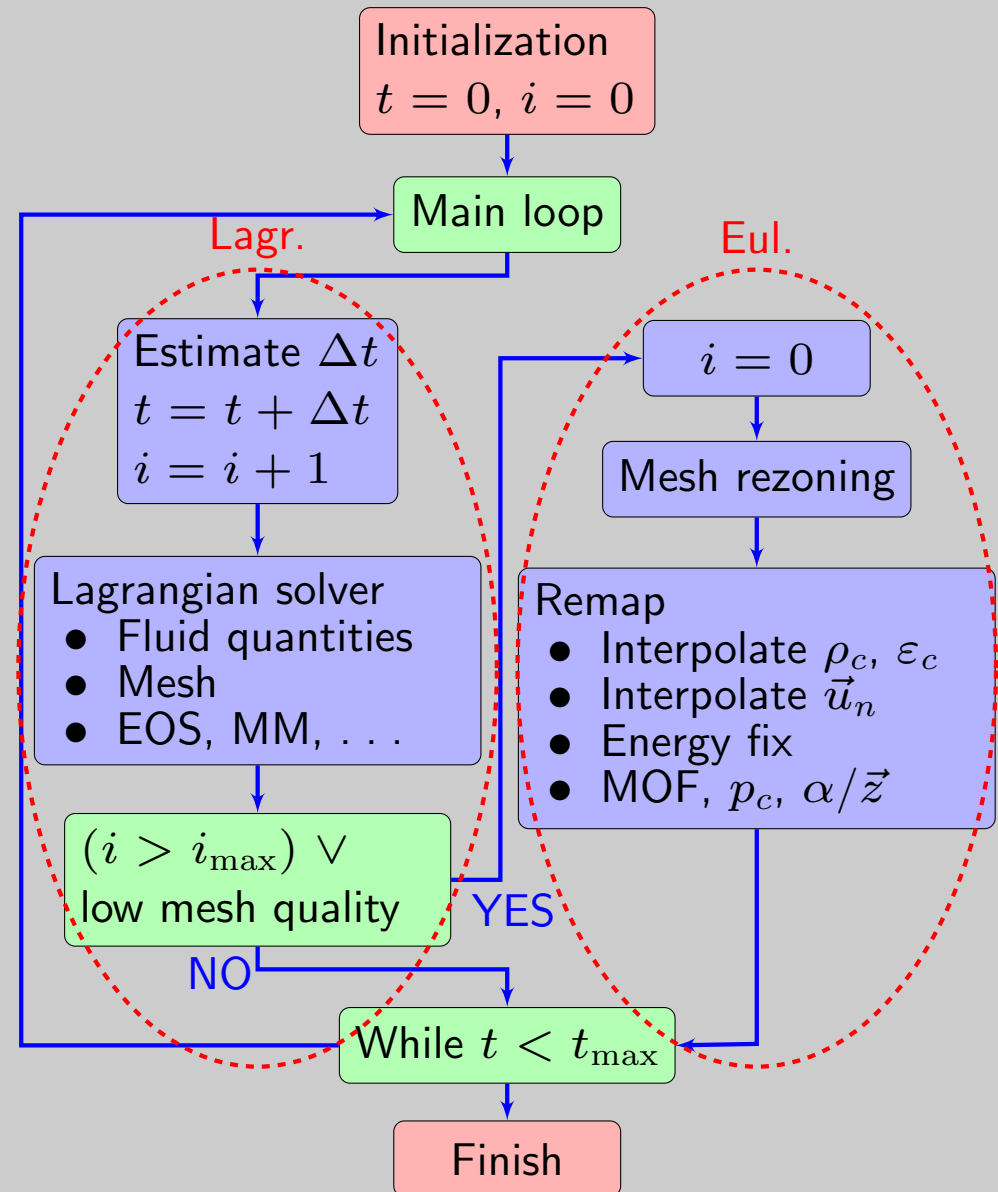


Arbitrary Lagrangian-Eulerian (ALE) methods

- Combination of both approaches – mesh following the fluid motion + guarantee its validity^[1].
- Recently very popular, present in many hydrodynamic laser/plasma codes.
- 2 types: direct vs. indirect ALE.
- Direct ALE methods:
 - Separate fluid and mesh velocities.
 - More complicated equations – formulation of fluid flow on differently moving mesh → convective term representing mass flux.
 - Filtering dangerous velocity components (shear flow, vortexes) out from the velocity field.

Indirect ALE methods

- Explicit separation of 3 steps:
 - 1) **Lagrangian step** = solver of PDEs, evolution of fluid quantities and mesh in time;
 - 2) **Rezoning** = untangling and smoothing of computational mesh, increasing its geometric quality;
 - 3) **Remap** = conservative interpolation of all quantities from Lagrangian to rezoned mesh.
- Rezone + remap = Eulerian part of the ALE algorithm (fluxes).
- Different strategies for triggering rezone/remap on (degeneracy, Eulerian, counter, . . .)



Example: Sedov blast wave

Euler

Lagrange

ALE20

Step 1: Lagrangian solver

- Solving the system of Euler equations in Lagrangian form:

$$\frac{D \rho}{D t} = -\rho \nabla \cdot \vec{w}, \quad (7)$$

$$\rho \frac{D \vec{w}}{D t} = -\nabla p, \quad (8)$$

$$\rho \frac{D \varepsilon}{D t} = -p \nabla \cdot \vec{w}, \quad (9)$$

with ODE for motion of mesh nodes

$$\frac{D \vec{x}}{D t} = \vec{w}, \quad (10)$$

and equation of state

$$p = \mathcal{P}(\rho, \varepsilon). \quad (11)$$

- Compatible Lagrangian scheme in staggered discretization (mimetic or support operators method)^[1].

Step 1: Lagrangian solver

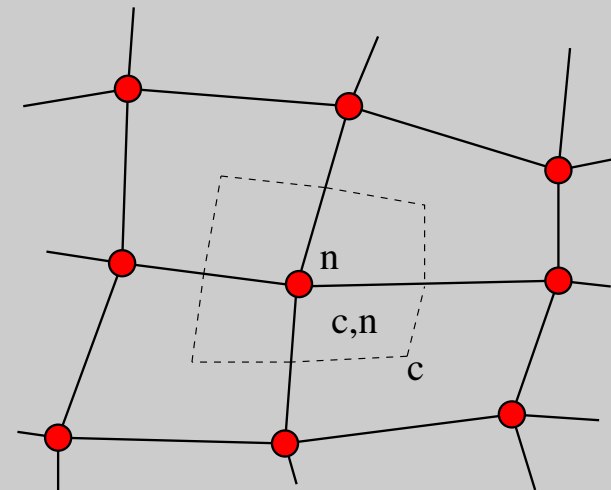
- Conservation of mass (7) – constant cell mass $m_c \Rightarrow$ automatically satisfied.
- Integration of momentum equation (8) over dual (nodal) volume V_n ,

$$m_n \left(\frac{D \vec{w}}{D t} \right)_n = \int_{V_n} \rho \frac{D \vec{w}}{D t} dV = - \int_{V_n} \nabla p dV \equiv \vec{F}_n^p. \quad (12)$$

- Forces on the right hand side can be written as

$$\vec{F}_n^p = \sum_{c \in C(n)} \vec{F}_{c,n}^p, \quad (13)$$

where $\vec{F}_{c,n}^p$ is force from cell c to node n due to pressure in c , can be computed from cell pressures and cell geometry.



- Left hand side – approximation of velocity derivative by finite difference:

$$\left. \frac{D \vec{w}}{D t} \right|_n \approx \frac{\vec{w}_n^{t^{n+1}} - \vec{w}_n^{t^n}}{\Delta t} \Rightarrow \vec{w}_n^{t^{n+1}} = \vec{w}_n^{t^n} + \frac{\Delta t}{m_n} \vec{F}_n^p. \quad (14)$$

Step 1: Lagrangian solver

- Motion of computational mesh nodes from (10) – again finite difference

$$\vec{x}_n^{t^{n+1}} = \vec{x}_n^{t^n} + \Delta t \vec{w}_n^{t^*}. \quad (15)$$

- Computation of new cell volumes $V_c^{t^{n+1}}$ from cell geometry.
- Update of cell densities

$$\rho_c^{t^{n+1}} = m_c / V_c^{t^{n+1}}. \quad (16)$$

- Total energy: internal + kinetic:

$$E = \sum_{\forall c} m_c \varepsilon_c + \sum_{\forall n} \frac{1}{2} m_n \|\vec{w}_n\|^2 = \sum_{\forall c} \left(m_c \varepsilon_c + \sum_{n \in N(c)} \frac{1}{2} m_{c,n} \|\vec{w}_n\|^2 \right), \quad (17)$$

where

$$m_c = \sum_{n \in N(c)} m_{c,n}, \quad m_n = \sum_{c \in C(n)} m_{c,n}. \quad (18)$$

Step 1: Lagrangian solver

- Conservation $\implies \partial E / \partial t = 0$, true if in each cell: $\partial E_c / \partial t = 0$,

$$m_c \frac{\partial \varepsilon_c}{\partial t} = - \sum_{n \in N(c)} m_{c,n} \|\vec{w}_n\| \frac{\partial \|\vec{w}_n\|}{\partial t} \equiv W_c. \quad (19)$$

- Substitution for velocity derivative from (12) \implies

$$m_c \frac{\partial \varepsilon_c}{\partial t} = W_c, \text{ where } W_c = - \sum_{n \in N(c)} \frac{m_{c,n}}{m_n} \vec{w}_n \cdot \vec{F}_{c,n}^p. \quad (20)$$

- W_c = released/removed heat in cell c due to its compression/expansion, can be explicitly computed.
- Energy update by central difference again,

$$\varepsilon_c^{t^{n+1}} = \varepsilon_c^{t^n} + \frac{\Delta t}{m_c} W_c. \quad (21)$$

- Due to this construction: exact energy conservation up to machine precision.

Step 1: Lagrangian solver

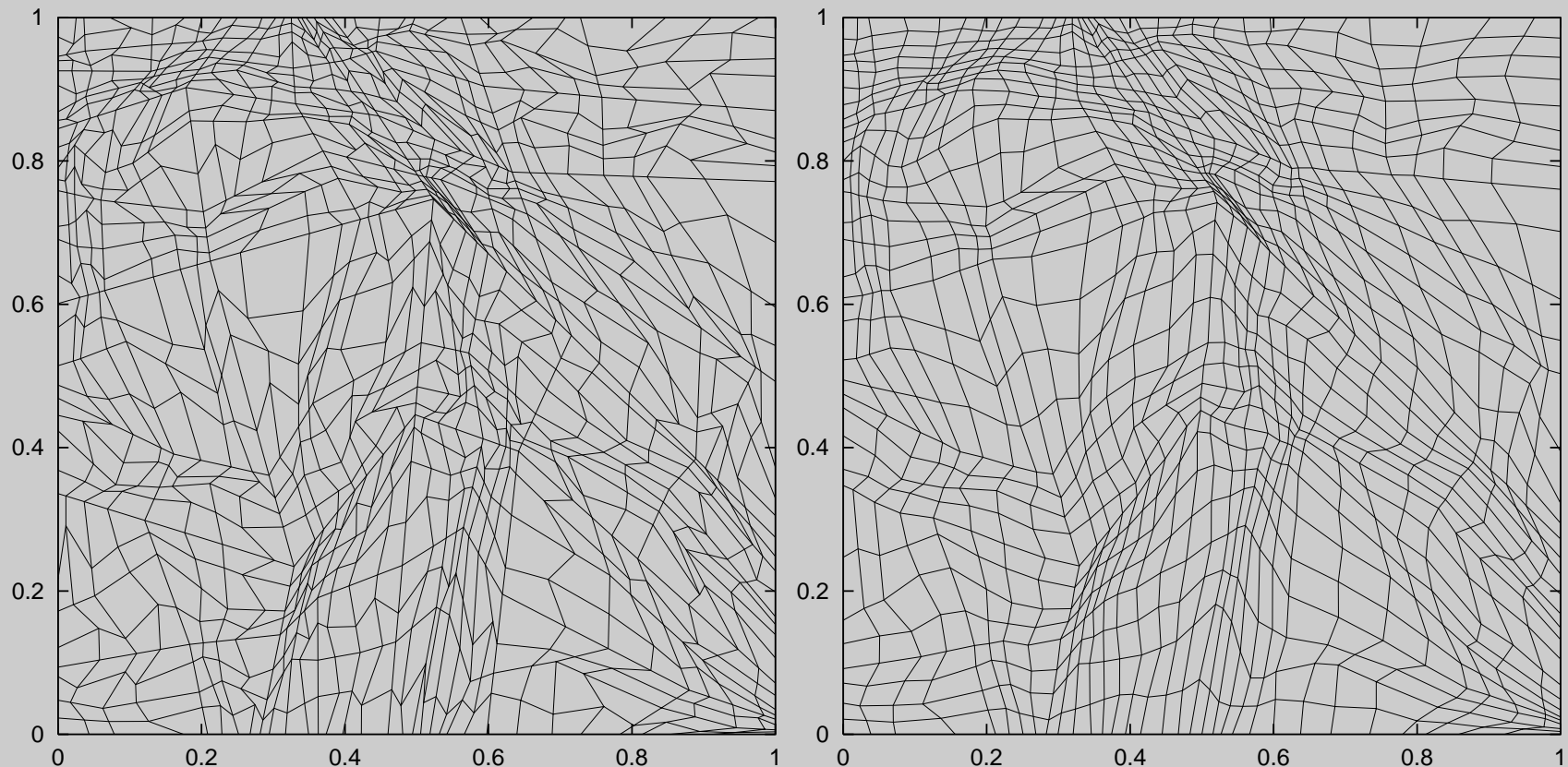
- Remaining only pressure update – from EOS (11),

$$p_c^{t^{n+1}} = \mathcal{P} \left(\rho_c^{t^{n+1}}, \varepsilon_c^{t^{n+1}} \right). \quad (22)$$

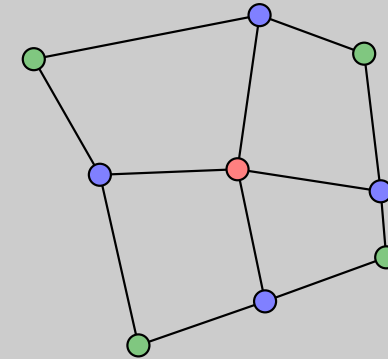
- Resulting scheme conservative in mass, momentum, and total energy.
- Usually used in two-step (predictor-corrector) form – prediction of pressure and velocity to $t^{n+1/2}$ → second order of accuracy.
- Next to pressure forces, other forces can be added:
 - Viscosity forces $\vec{F}_{c,n}^q$ – stabilization of the scheme (elimination of oscillations) at shocks, several models^[1,2].
 - Subzonal-pressure forces $\vec{F}_{c,n}^{dp}$ – finer pressure discretization, reducing unwanted mesh degeneracies (hourglass)^[3].
 - Other forces due to physical modes, such as gravity forces, . . .

Step 2: Mesh rezoning

- Mesh rezoning = mesh untangling (making it valid) and smoothing (increasing its geometric quality).
- To avoid excessive diffusion of the solution in the following remapping step – move only nodes needed to move, and as little as possible.



Step 2: Mesh rezoning



- Many rezoning methods.
- In realistic computations – efficient methods (3D), e.g. Laplace or Winslow.
- Laplace: new positions as weighted average,

$$\tilde{\vec{x}}_{i,j} = \sum_{k,l=-1,1} w_{i+k,j+l} \vec{x}_{i+k,j+l}, \text{ where } \sum_{k,l=-1,1} w_{i+k,j+l} = 1. \quad (23)$$

- Winslow^[1]: based on solving of elliptic PDEs in logical directions,

$$\tilde{\vec{x}}_{i,j} = \frac{1}{2(\alpha^k + \gamma^k)} \left(\alpha^k (\vec{x}_{i,j+1} + \vec{x}_{i,j-1}) + \gamma^k (\vec{x}_{i+1,j} + \vec{x}_{i-1,j}) - \frac{1}{2} \beta^k (\vec{x}_{i+1,j+1} - \vec{x}_{i-1,j+1} + \vec{x}_{i-1,j-1} - \vec{x}_{i+1,j-1}) \right), \quad (24)$$

where coefficients $\alpha = x_\xi^2 + y_\xi^2$, $\beta = x_\xi x_\eta + y_\xi y_\eta$, $\gamma = x_\eta^2 + y_\eta^2$, and where (ξ, η) are the logical coordinates.

- More advanced methods – eg. CN minimization, RJM^[2]. For untangling – modified CN minimization, feasible set^[3].

Step 3: Quantity remapping

- Remap = **conservative** interpolation of all fluid quantities from old (Lagrangian) computational mesh to new (rezoned) one.
- **Given:** values of given quantity (e.g. density ρ_c) in the cell centroid $\vec{x}_c = \frac{1}{V_c} \int_c \vec{x} dV$, $V_c = \int_c 1 dV$.
- Understood as mean values of unknown underlying density function $\rho(\vec{x})$:

$$m_c = \int_c \rho(\vec{x}) dV, \quad \rho_c = m_c/V_c. \quad (25)$$

- **Goal:** compute new masses

$$m_{\tilde{c}} \approx \int_{\tilde{c}} \rho(\vec{x}) dV \quad (26)$$

and mean values $\rho_{\tilde{c}} = m_{\tilde{c}}/V_{\tilde{c}}$ in the rezoned cells \tilde{c} .

Step 3: Quantity remapping

- Requirements:
 - **Conservation**: $\sum_c m_c = \sum_{\tilde{c}} m_{\tilde{c}}$.
Solving conservation laws, do not want to spoil it.
 - **Accuracy**: $\rho_{\tilde{c}} \approx \rho(\tilde{c})$.
Mean value should be close to the function value in the cell centroid.
 - **Linearity-preservation**: $\rho(\vec{x})$ linear $\Rightarrow \rho_{\tilde{c}} = \rho(\vec{x}_{\tilde{c}})$.
Implies second order of convergence.
 - **Consistency (continuity)**: $c = \tilde{c} \Rightarrow \rho_c = \rho_{\tilde{c}}$.
Do not want to change value if cell did not change.
 - **Bound-preservation**: $\rho_c^{\min} \leq \rho_{\tilde{c}} \leq \rho_c^{\max}$, where $\rho_c^{\min} = \min_{c' \in C(c)} \rho_{c'}$.
Only interpolation \Rightarrow do not want to create new extrema.

Step 3: Quantity remapping – Reconstruction

- First phase – piece-wise linear reconstruction of density function (2D):

$$\rho(x, y)|_c \approx \rho_c(x, y) = \rho_c + \left(\frac{\partial \rho}{\partial x}\right)_c (x - x_c) + \left(\frac{\partial \rho}{\partial y}\right)_c (y - y_c). \quad (27)$$

- Slopes $(\partial \rho / \partial x)_c$, $(\partial \rho / \partial y)_c$:

- Integral average over super-cell:

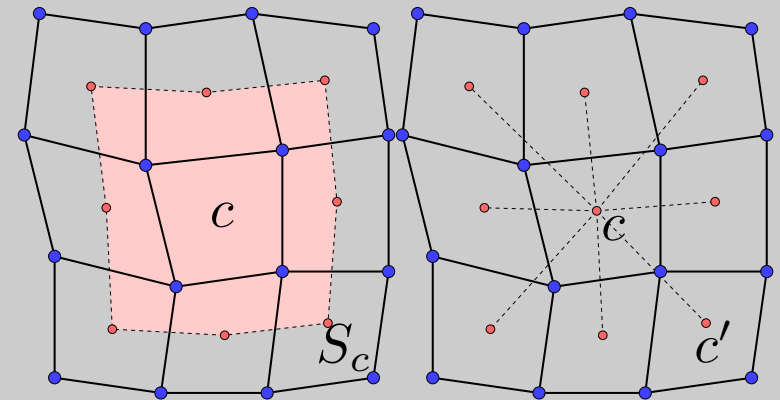
$$\left(\frac{\partial \rho}{\partial x}\right)_c \approx \frac{1}{V_{S_c}} \int_{S_c} (\partial \rho / \partial x) dV.$$

- Minimization (LS) of error functional:

$$\left(\frac{\partial \rho}{\partial x}\right)_c \approx \arg \min \Phi(\partial \rho / \partial x, \partial \rho / \partial x),$$

$$\Phi(\partial \rho / \partial x, \partial \rho / \partial x) = \sum_{c' \in C(c)} \|\rho(\vec{x}_{c'})|_c - \rho_{c'}\|^2.$$

- Other possibilities.

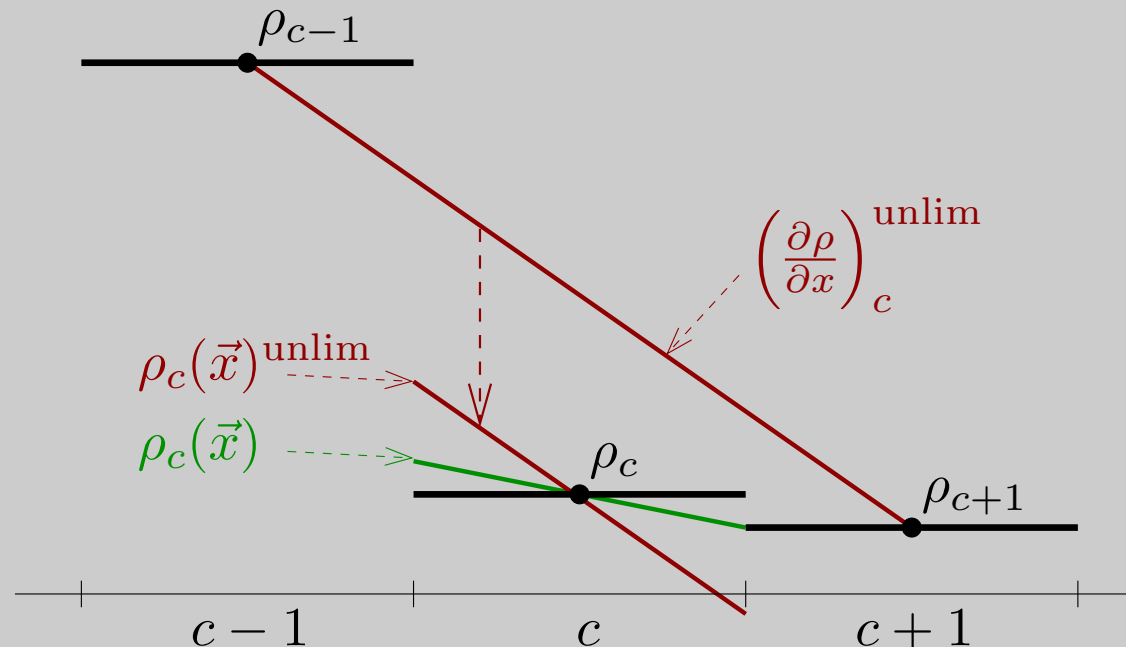


Step 3: Quantity remapping – Reconstruction

- Usually with limiter, e.g. Barth-Jespersen^[1]:

$(\partial\rho/\partial x)_c = \Psi_c (\partial\rho/\partial x)_c^{\text{unlim}}$, where $\Psi_c = \min_{c' \in C(c)} \Psi_{c,n}$, and

$$\Psi_{c,n} = \begin{cases} \min\left(1, \frac{\rho_c^{\text{max}} - \rho_c}{\rho_c^{\text{unlim}(n)} - \rho_c}\right) & \text{for } \rho_c^{\text{unlim}(n)} - \rho_c > 0 \\ \min\left(1, \frac{\rho_c^{\text{min}} - \rho_c}{\rho_c^{\text{unlim}(n)} - \rho_c}\right) & \text{for } \rho_c^{\text{unlim}(n)} - \rho_c < 0 \\ 1 & \text{for } \rho_c^{\text{unlim}(n)} - \rho_c = 0. \end{cases}$$



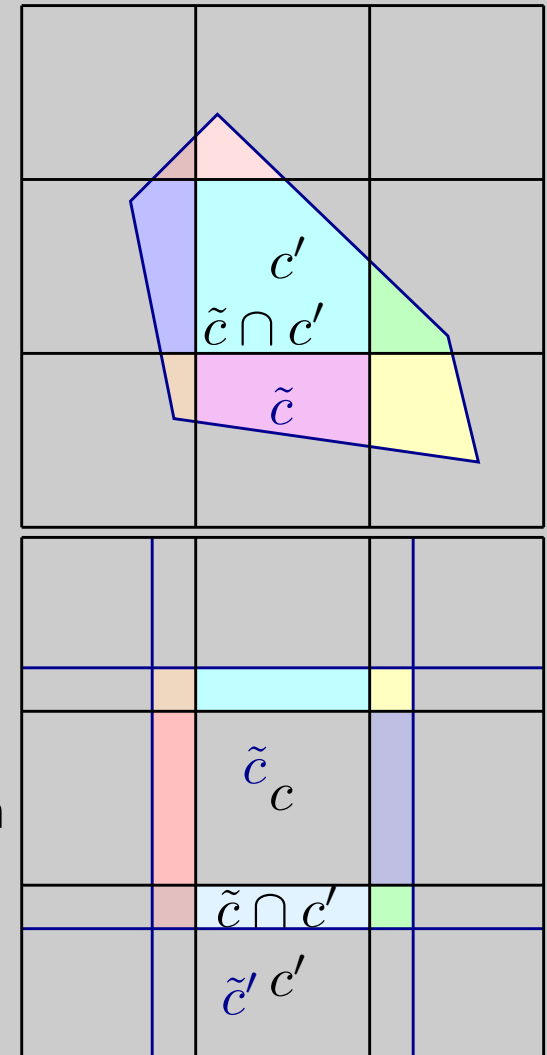
Step 3: Quantity remapping – Exact integration

- Most natural method based on cell intersections:

$$m_{\tilde{c}} = \int_{\tilde{c}} \rho(\vec{x}) dV = \sum_{\forall c' \tilde{c} \cap c'} \int \rho(\vec{x}) dV \approx \sum_{\forall c' \tilde{c} \cap c'} \int \rho_{c'}(\vec{x}) dV.$$

- General geometry \Rightarrow global remap.
- Conservation obvious, limiter \Rightarrow local extrema.
- Same topology \Rightarrow can be formulated in flux form^[1]:

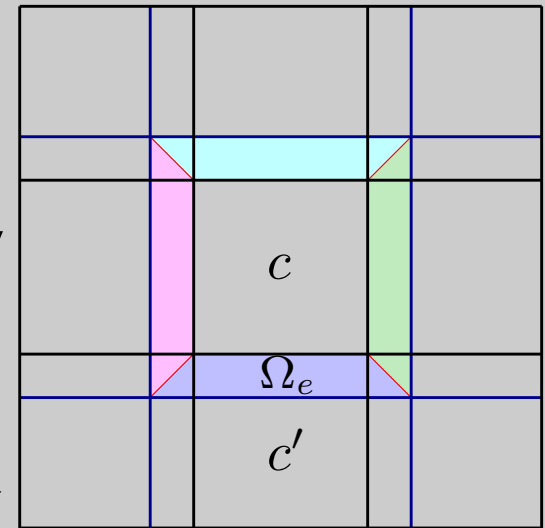
$$m_{\tilde{c}} = m_c + \sum_{c' \in C(c)} F_{c' \rightarrow c}^m, \quad F_{c' \rightarrow \tilde{c}}^m = \int_{\tilde{c} \cap c'} \rho_{c'}(\vec{x}) dV - \int_{\tilde{c}' \cap c} \rho_c(\vec{x}) dV.$$
- Flux form \Rightarrow conservation guaranteed \Rightarrow more freedom in flux construction.
- Problems: computationally expensive, robustness, 3D.



Step 3: Quantity remapping – Approximate integration

- Flux approximated using swept regions^[1]:

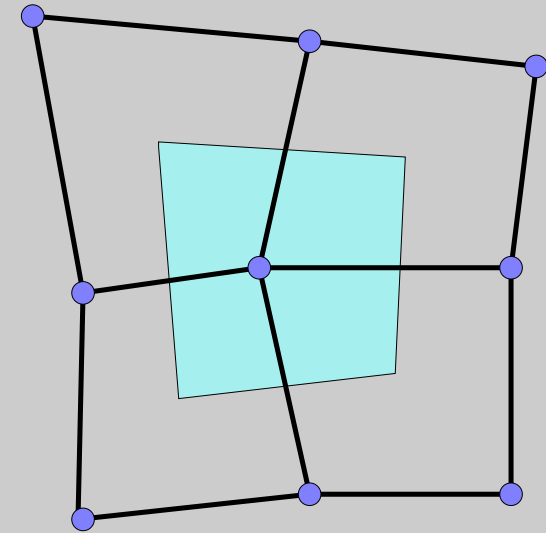
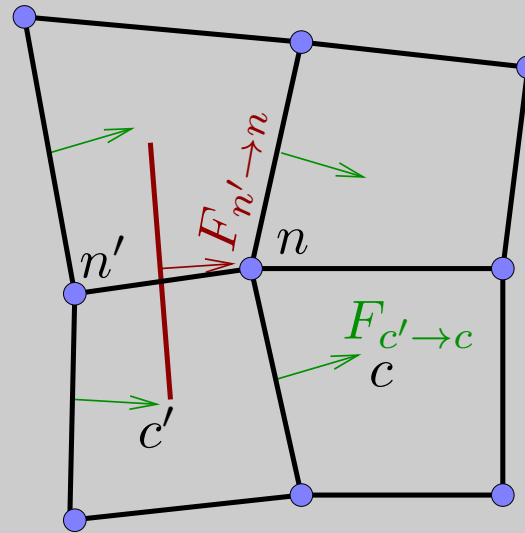
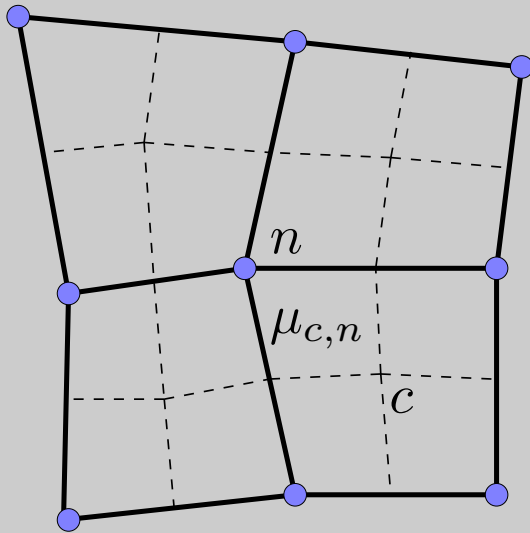
$$m_{\tilde{c}} = m_c + \sum_{e \in \mathcal{E}(c)} F_e^m, \text{ where } F_e^m = \int_{\Omega_e} \rho_{c^*}(\vec{x}) dV, c^* = c/c'.$$
- No intersections needed \Rightarrow less computationally expensive, robustness.
- **Problem:** in certain parts of new cells (corner flux, rotating edge), approximation from wrong cell is used \Rightarrow local bound violation.
- Several options for fixing this:
 - A-posteriori mass redistribution (repair)^[2];
 - Flux Corrected Transport (FCT)^[3];
 - Multi-dimensional Optimal Order Detection (MOOD)^[4];
 -
- Difficult generalization for multi-material case.



Remap of all fluid quantities

- Up to now – only remap of ρ , m .
- Remap of ε – similar as density.
- Pressure – usually computed from EOS, but can be remapped too.
- Remap of \vec{w} – simple in cell-centered methods (same manner), more complicated in staggered discretization.
- Kinetic energy computed from remapped velocities – non-linear \rightarrow violation of kinetic energy conservation \Rightarrow wrong shock speeds, wrong plateau height, . . .
- Typically treated by **energy fix**^[1]: remap kinetic energy independently and distribute its discrepancy to internal energy.
- Several options for velocity remap.

Remap of all fluid quantities



- Double-fine mesh^[1].
- Inter-nodal fluxes^[2].
- Remap on dual cells^[3].

• Simplest way:

- $\mu_{c,n} = m_{c,n} u_n$,
- remap $\mu_{c,n} \rightarrow \mu_{\tilde{c},\tilde{n}}$,
- $u_{\tilde{n}} = \sum_{c' \in C(n)} \mu_{\tilde{c}',\tilde{n}} / m_{\tilde{n}}$.

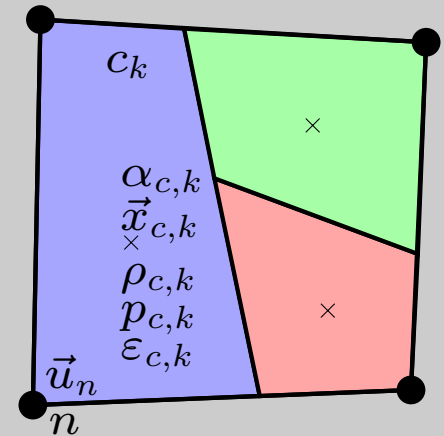
- Interpolation of $F_{n' \rightarrow n}^m$ from $\forall F_{c' \rightarrow c}^m$, μ flux:
 $F_{n' \rightarrow n}^\mu = u_{n' \rightarrow n}^{\text{rec}} F_{n' \rightarrow n}^m$.

- $$u_{\tilde{n}} = \frac{\mu_n + \sum_{n' \in N(n)} F_{n' \rightarrow n}^\mu}{m_{\tilde{n}}}.$$

- The rest same as for other quantities.

Multi-material ALE

- Lagrangian simulation – different materials in different cells, remain there for the whole simulation.
- ALE \Rightarrow mixing unavoidable \Rightarrow numerical interface diffusion, useless EOS, . . .
- Solution: multi-material ALE.
- Concentrations \times splitting of cell c to polygons c_k representing particular materials k , thermodynamic quantities separately for each material.
- Additional: material quantities – relative volume (volume fraction) $\alpha_{c,k}$, eventually approximate material position (centroid) $\vec{x}_{c,k}$.
- Splitting of c to $c_k =$ material reconstruction^[1]: Volume of Fluid (VOF)^[2], Moment of Fluid (MOF)^[3], . . .



Multi-material ALE – Differences

- In Lagrangian step – additional model for material interaction (closure model) defining interface motion \rightarrow evolution of $\alpha_{c,k}$.
- In rezone – no difference. Methods minimizing rezone at material interfaces.
- In remap – generalization of exact integration \rightarrow instead of intersection with original cell c , so intersections with all its material polygons $c_k^{[1]}$.
- Next to remap of standard fluid quantities, remap of $\alpha_{c,k}$ and $\vec{x}_{c,k}$.
- Reconstruction/remap of velocity vector must be performed in a consistent way, otherwise can lead to conservation violation due to non-linearity of kinetic energy^[2], or symmetry violation of velocity field^[3].

Physical aspects – Model

- Laser plasma – simplest approximation by modification of energy equation:

$$\frac{d\rho}{dt} = -\rho \nabla \cdot \vec{w}, \quad (28)$$

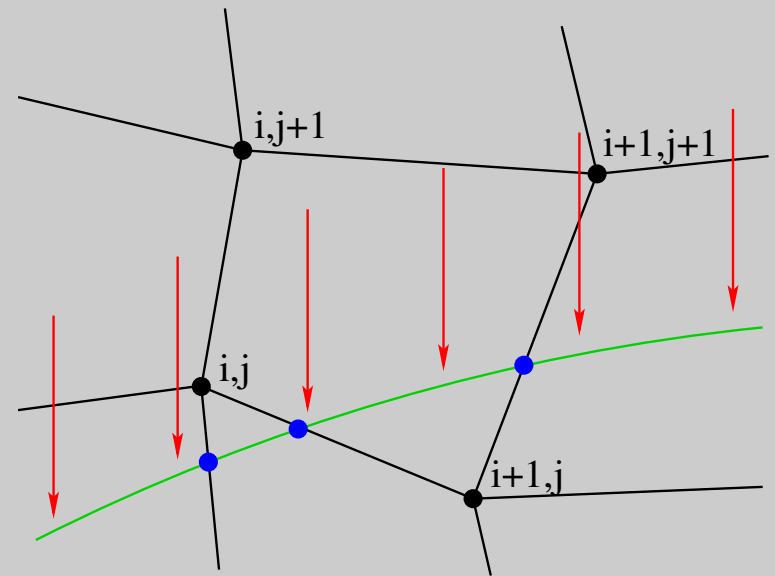
$$\rho \frac{d\vec{w}}{dt} = -\nabla p, \quad (29)$$

$$\rho \frac{d\varepsilon}{dt} = -p \nabla \cdot \vec{w} + \nabla \cdot (\kappa \nabla T) - \nabla \cdot \vec{I}, \quad (30)$$

where T is temperature, κ is heat conductivity coefficient, and \vec{I} is laser beam intensity profile.

Physical aspects – Laser absorption

- Simple model of laser absorption on the critical surface^[1].
- Laser radiating from upwards – $\vec{I} = (0, -I_z(t, r))$, Gaussian profile.
- On each edge – projection of intensity to the normal direction \vec{I}_e .
- Interpolation of nodal density from neighbors.
- Density in all cell nodes sub- or super-critical $\Rightarrow (D \vec{I})_c = 0$.
- Mixed $\Rightarrow (D \vec{I})_c = \frac{1}{V_c} \sum_{e \in \delta c} L^s(e) \vec{I}_e$,
 $L^s(e)$ – subcritical edge length,
 \vec{I}_e – projected intensity along edge.
- Equation of absorption: $\rho \frac{d\varepsilon}{dt} + p \nabla \cdot \vec{w} = -C_A \nabla \cdot \vec{I}$, C_A – coefficient.



Physical aspects – Laser absorption

- Problems – C_A needed from user + full absorption in one cell leading to series of “cell explosions”.
- Several more advanced models.
- Raytracing^[1] – explicit tracking of each single ray in the domain, including its refractions on the cell boundaries.
- Wave-based models employing stationary solution of Maxwell equations^[2].

Physical aspects – Heat conductivity

- Represented by parabolic term in the energy equation.
- Separated by operator splitting to the form $\rho \varepsilon_t = \nabla \cdot (\kappa \nabla T)$, transformed to temperatures $T_t = \frac{1}{\rho \varepsilon_T} \nabla \cdot (\kappa \nabla T)$.
- Solving using support operators method^[1].
- Temperature derivative of energy ε_T computed numerically.
- Classical Spitzer-Harm heat conductivity coefficient

$$\kappa = 20 \left(\frac{2}{\pi} \right)^{3/2} \frac{k^{7/2}}{\sqrt{m_e} e^4} \delta_{ee} \frac{T^{5/2}}{Z \ln \Lambda} \quad (31)$$

corrected by electron-electron collision term $\delta_{ee} = 0.095 \frac{Z+0.24}{1+0.24Z}$, where k is Boltzmann constant, m_e is the electron mass unit, e is the electron charge, Z is the plasma mean ion charge, and $\ln \Lambda$ is the Coulomb logarithm.

Physical aspects – Heat conductivity

- Green/Gauss theorems express integral properties of operators:

- Generalized gradient $\vec{W} = \vec{G}T = -\kappa \nabla T$

- Extended divergence $\vec{D} \vec{W} = \begin{cases} \nabla \vec{W} & \text{in } V \\ -(\vec{W}, \vec{n}) & \text{on } \partial V \end{cases}$

- Mimetic discrete operators G, D have the same discrete integral properties, namely gradient is adjoint of divergence $G = D^*$.
- Fully implicit scheme in time $(T^{n+1} - T^n)/\Delta t + D G T^{n+1} = 0$.
- Explicit not suitable: CFL \Rightarrow many steps per 1 Lagrangian step.
- Matrix of global system is symmetric and positive definite – conjugate gradient method.
- Exact on piecewise linear solutions, otherwise it is second order accurate in space. Works well on bad quality meshes, allows discontinuous diffusion coefficient.

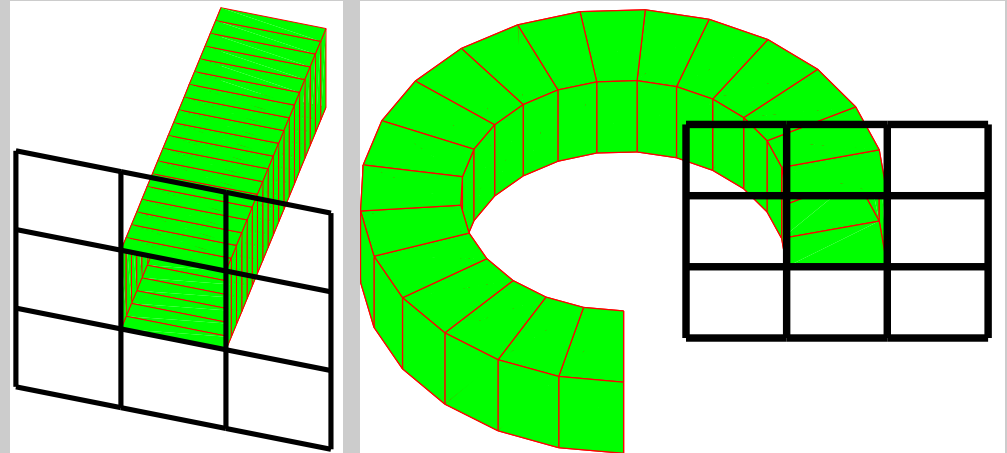
Physical aspects – Heat flux limiter

- Standard methods can provide higher heat flux \vec{W} than physically feasible – need to limit it.
- Compare sizes of heat fluxes with local free stream limit $W^{lim} = f^{max} \frac{k}{m_u} \sqrt{\frac{k}{m_e} \frac{Z\rho}{A} T^{3/2}}$, where the coefficient $f^{max} \in (0.05, 0.3)$ (between 5% and 30% of the physical limit).
- Compute values $c = \frac{W^{lim}}{|\vec{W}|}$, and renormalize the conductivity coefficient $\tilde{\kappa} = c\kappa$ in each cell.
- The conductivity equation is then solved for the second time with new $\tilde{\kappa}$, ensuring the limit is not exceeded.
- Need to solve the global system twice \rightarrow new temperatures/energies more realistic.

Physical aspects – EOS

- EOS crucial, strongly affects realistic simulations.
- Ideal gas for simple fluid test, reasonably valid in low-density corona.
- Realistic EOSes – significantly more computationally expensive, often tabulated.
- Quotidian EOS (QEOS)^[1] for real plasma – Thomas-Fermi theory for electrons and Cowan model for ions.
- Sesame EOS^[2] – tables of measured values + several material theories providing interpolation techniques.
- Various modifications – such as Badger or FEOS.
- HerEOS^[3] – library for Hermite interpolation of tabulated data.

Physical aspects – ALE in cylindrical geometry

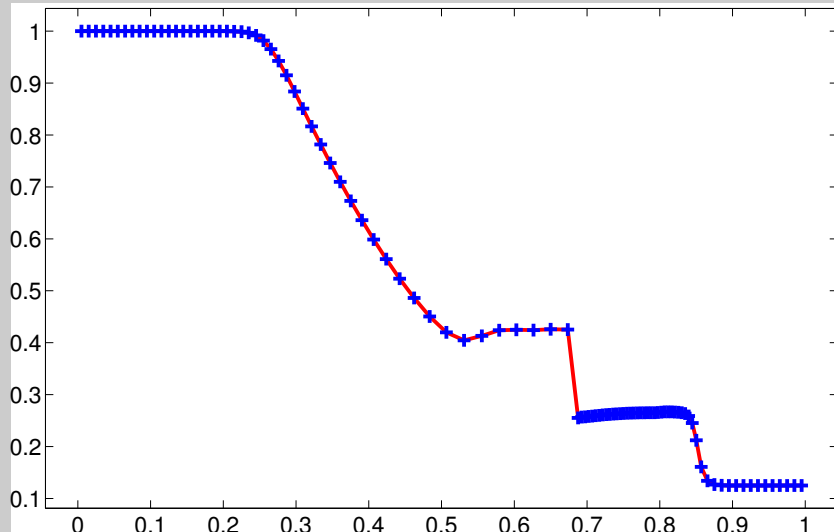


- Many laser-related processes are cylindrically symmetrical, 2D code with cylindrical geometry well approximates 3D reality.
- Switching to cylindrical geometry = adding r factor into all integrals – different volumes, centroids.
- Lagrangian solver – adding r factor leads to Control Volume scheme: integration mainly in forces.
- Mesh rezoning – no change, done as in Cartesian case.
- Remap: r arises during integration.

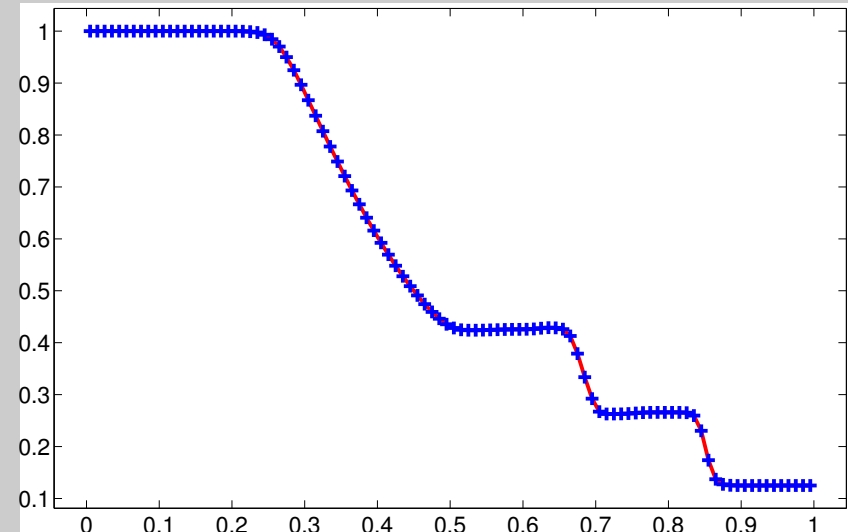
Physical aspects – Others

- Many other models can be needed/usefull:
 - Two-temperature model – separate electron/ion temperatures → two energy equations + heat exchange term. More realistic for non-ideal plasma.
 - Phase transition model – taking into account latent heat of melting and evaporation, important for interaction with solid targets.
 - Non-local energy transport – represents long-distance transfer of energy due to material radiation.
- Most of described methods implemented in Prague ALE (PALE) code – Fortran, 2D Cartesian/cylindrical geometry, staggered ALE, realistic EOSes, laser absorption, heat conductivity + limiter, two-temperature model, . . .
- Simulations of laser/target interactions, experiments at PALS or ELI.

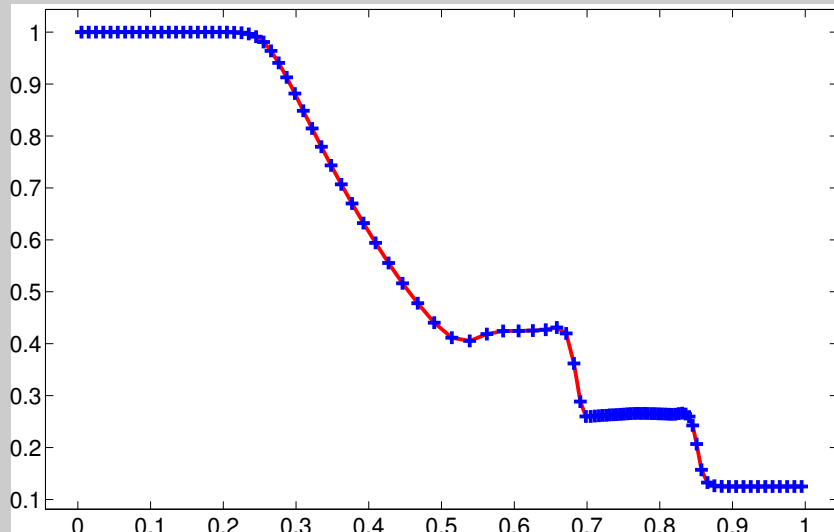
Fluid examples: 1D Sod problem



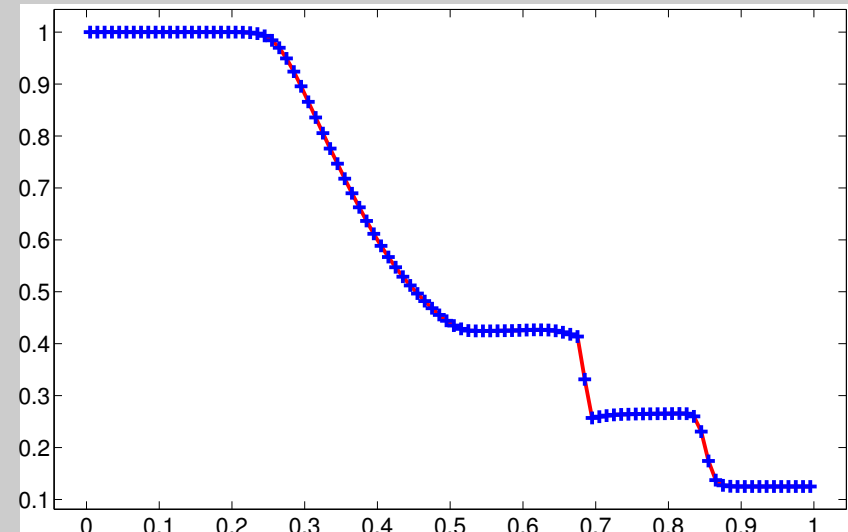
Lagrangian



Eulerian



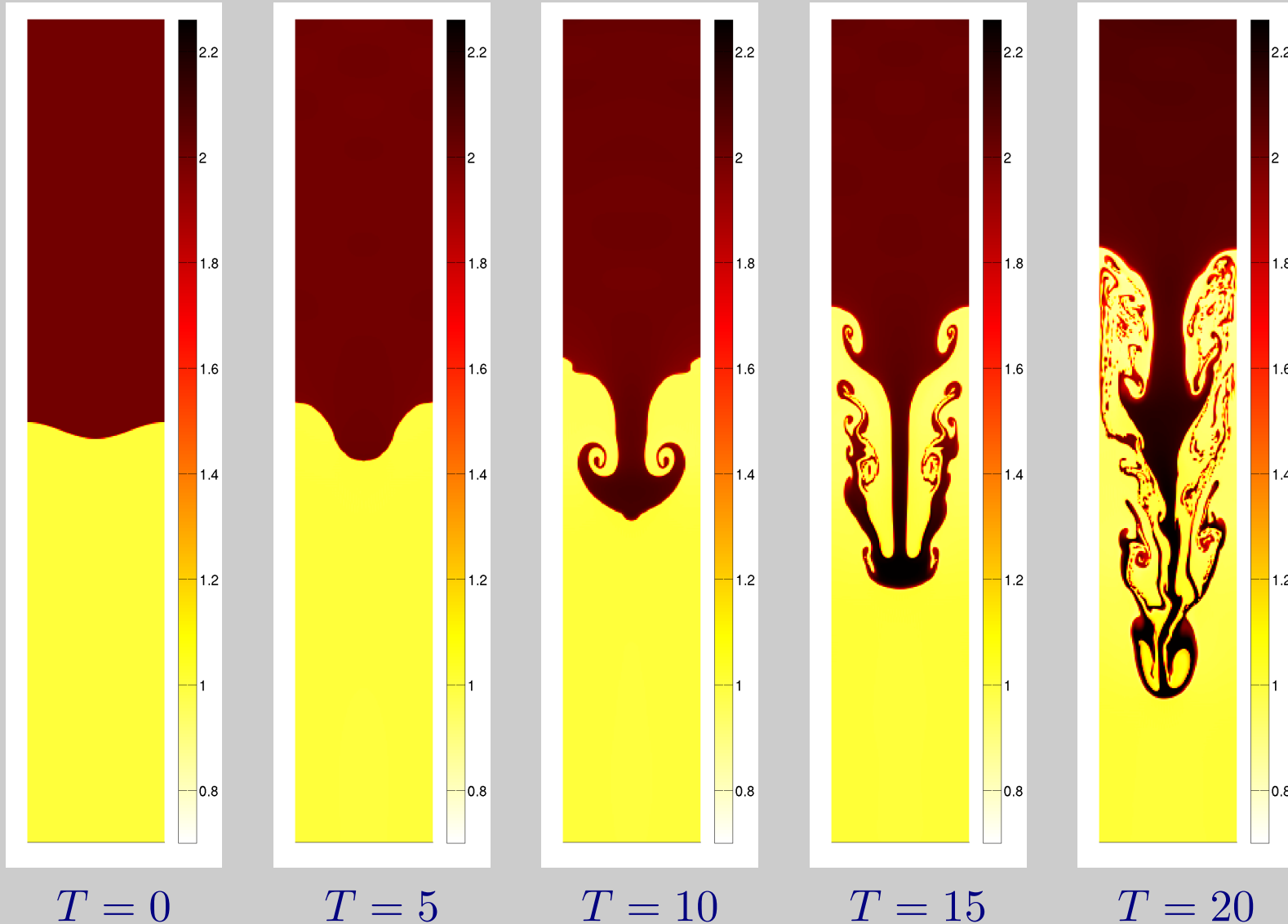
ALE 10



MM Eulerian

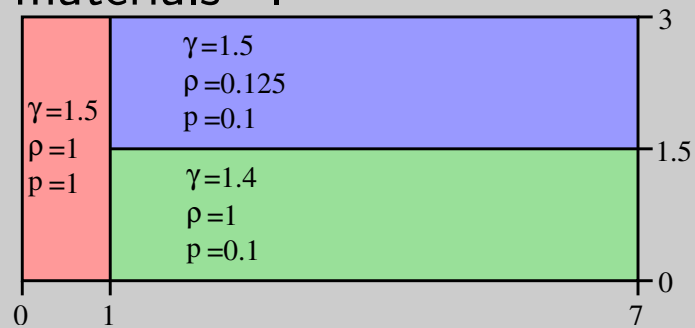
Fluid examples: Rayleigh-Taylor instability

100 × 600 mesh, MM, Eulerian regime^[1].

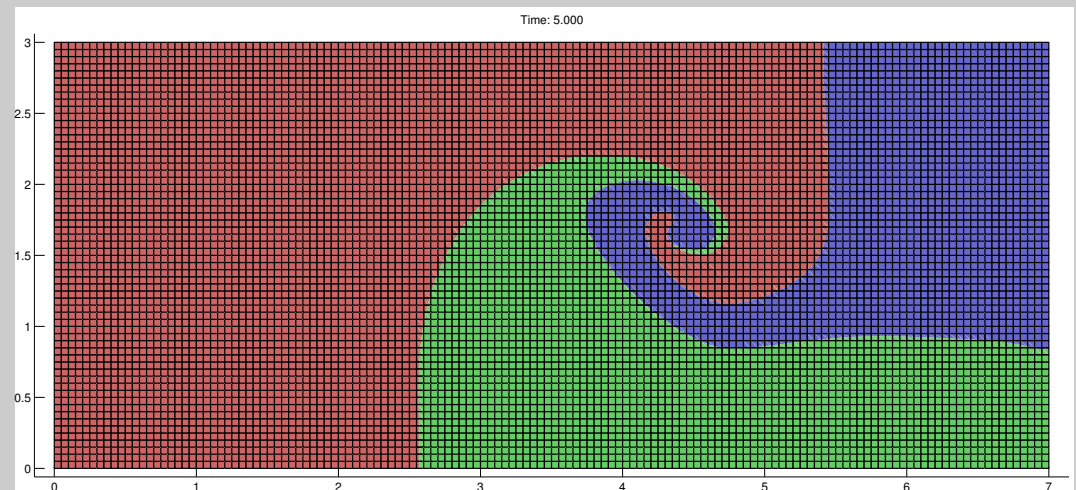


Fluid examples: Triple point problem

- Interfaces among three materials^[1].

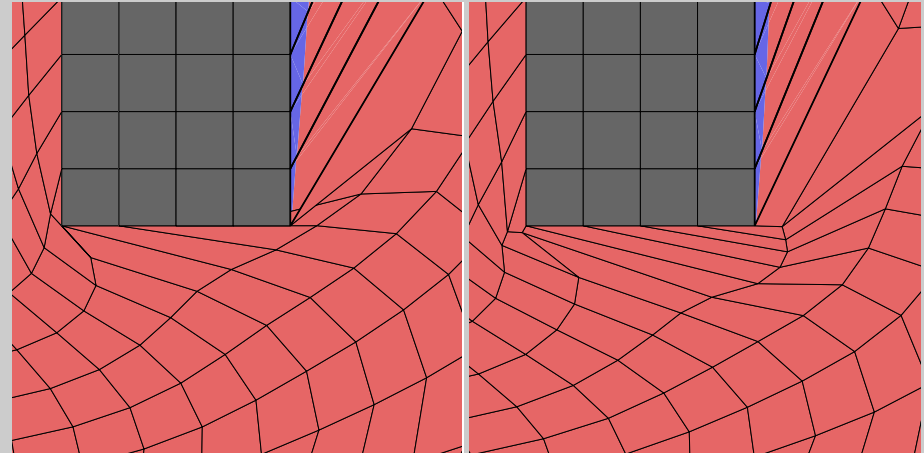


- Higher pressure generates shock, different properties of right materials \Rightarrow vortex.
- Eulerian run, thin filaments.



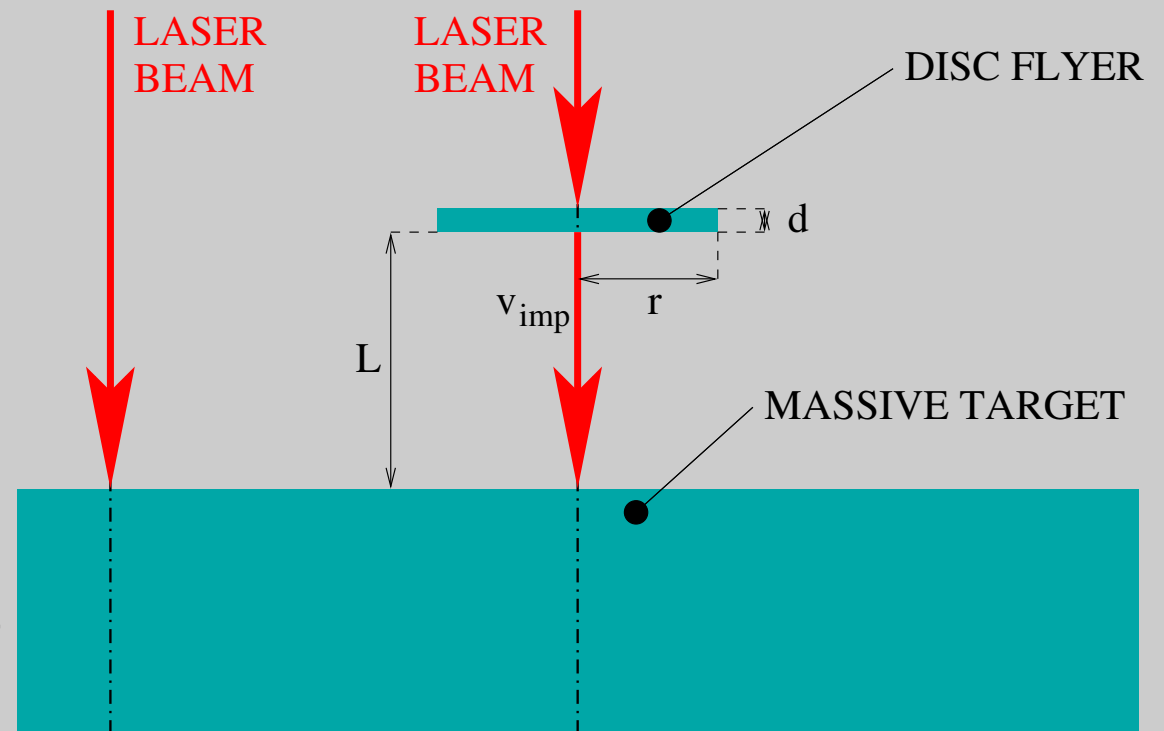
Fluid examples: Jet through a hole in a wall

- Hole in a wall^[1] (inactive cells), larger left pressure \Rightarrow jet.
- Deformation of cells around the hole, ALE simulation failure.
- Feasible-set mesh untangling \Rightarrow increased robustness.

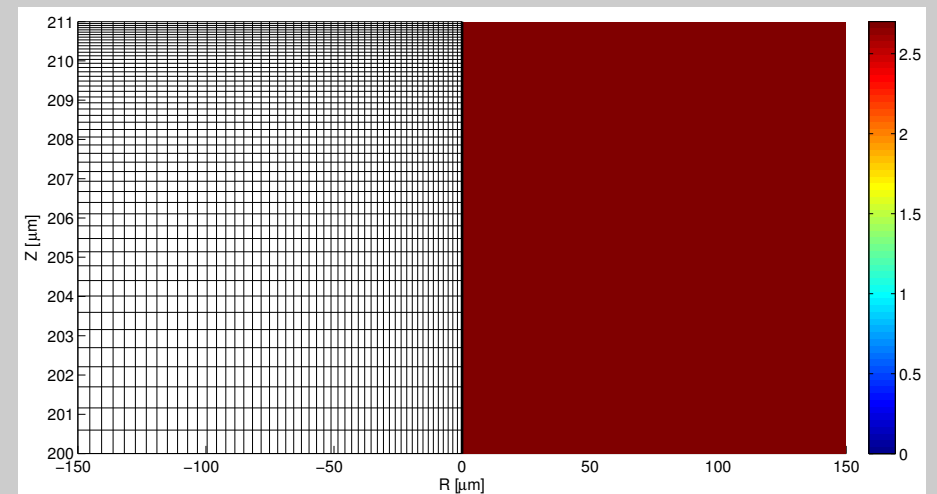
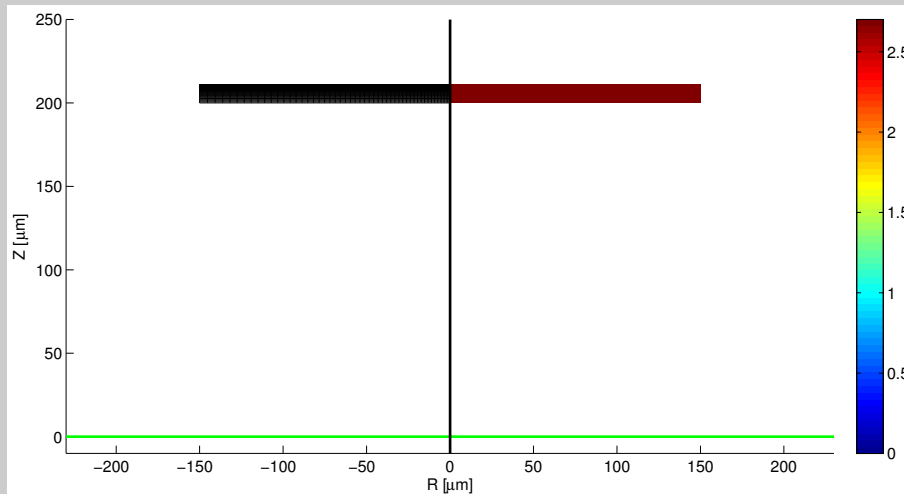


Laser examples: Disc impact

- Simulation inspired by experiments on PALS system^[1].
- Laser evaporates disc target, acceleration to tens/hundreds km/s^[2].
- Impact to massive target.
- Melting and evaporation of material, crater formation.

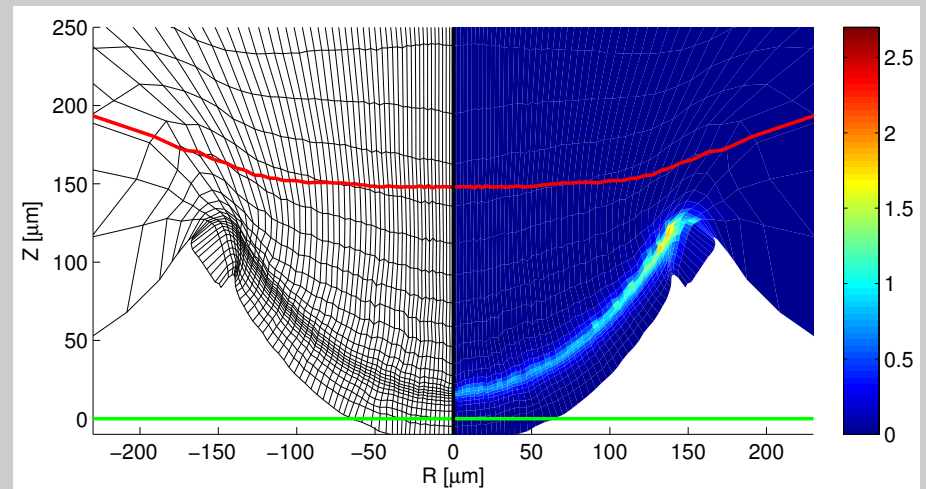
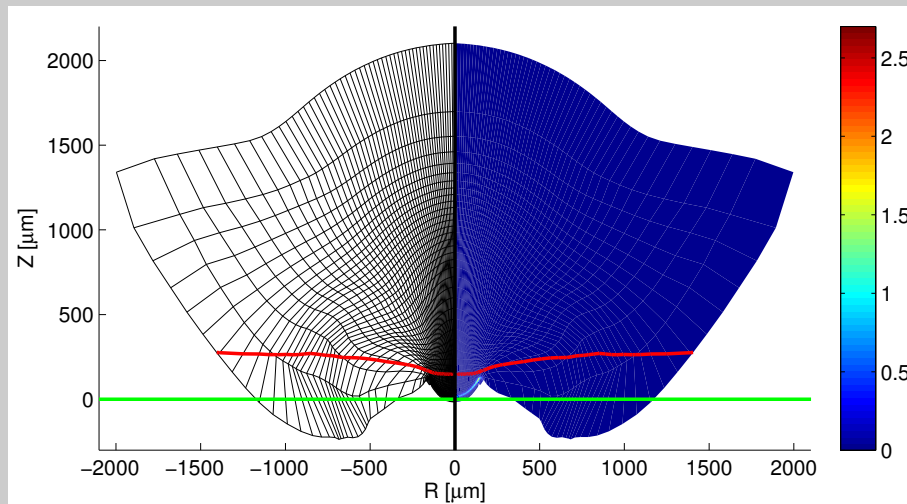


Laser examples: Disc impact – 1) ablative acceleration

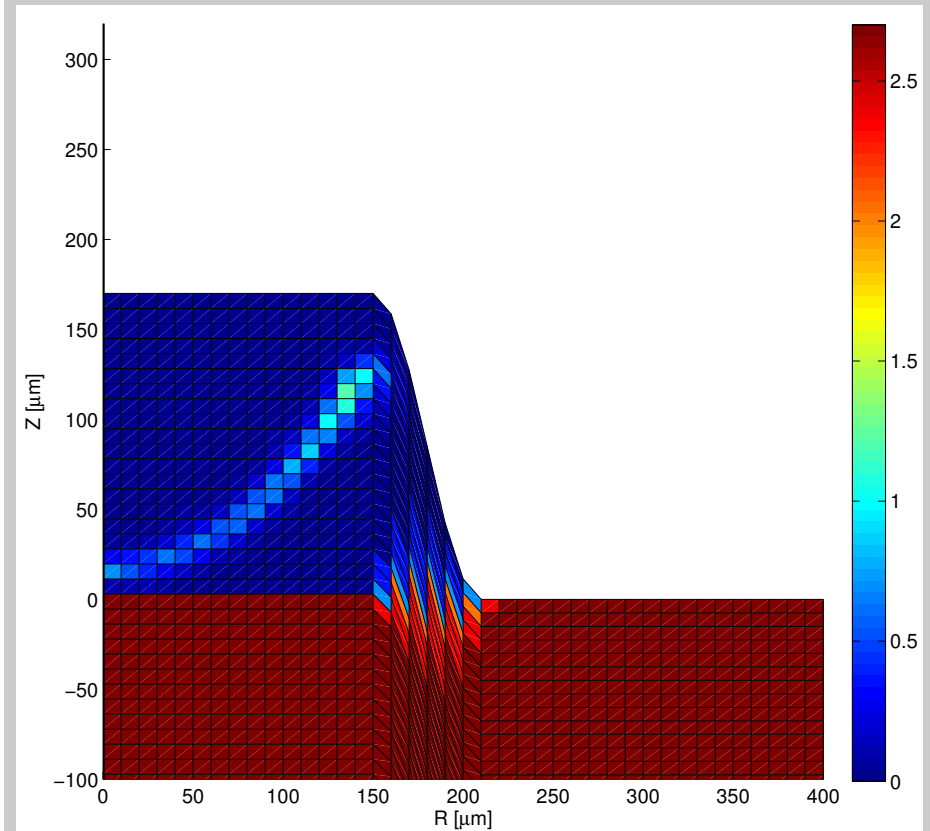
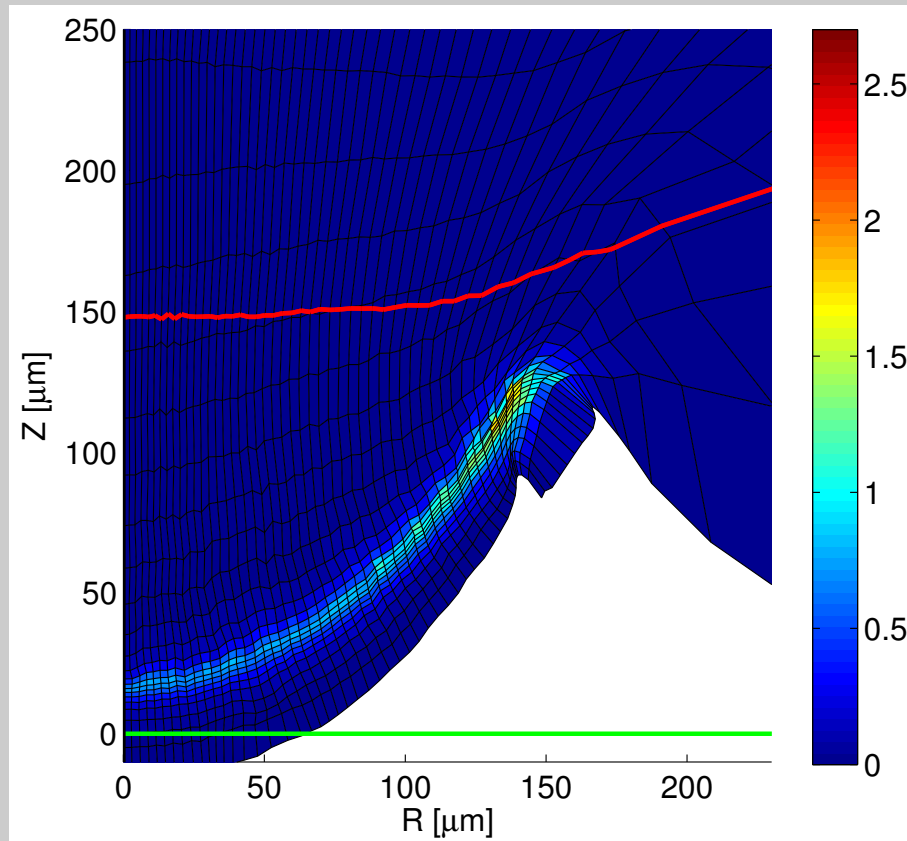


- Geometrical computational mesh, in disc only.
- Laser absorption, material evaporation upwards.
- Massive part of the disc accelerated downward due to ablation (momentum conservation).

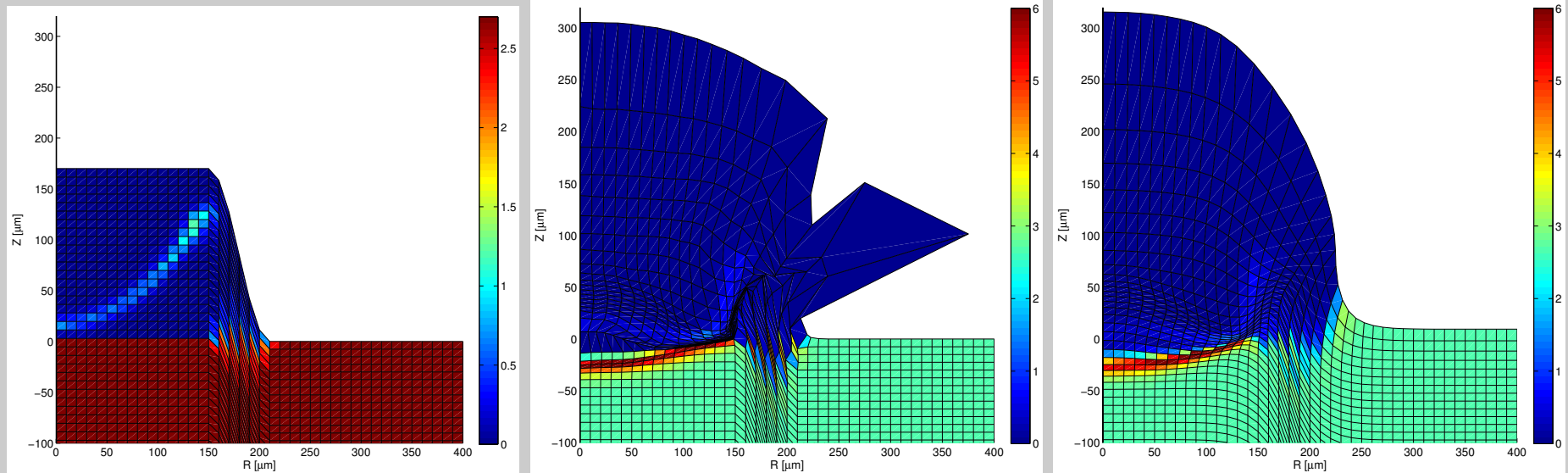
Laser examples: Disc impact – 1) ablative acceleration



Laser examples: Disc impact – 2) interpolation



Laser examples: Disc impact – 3) impact, crater



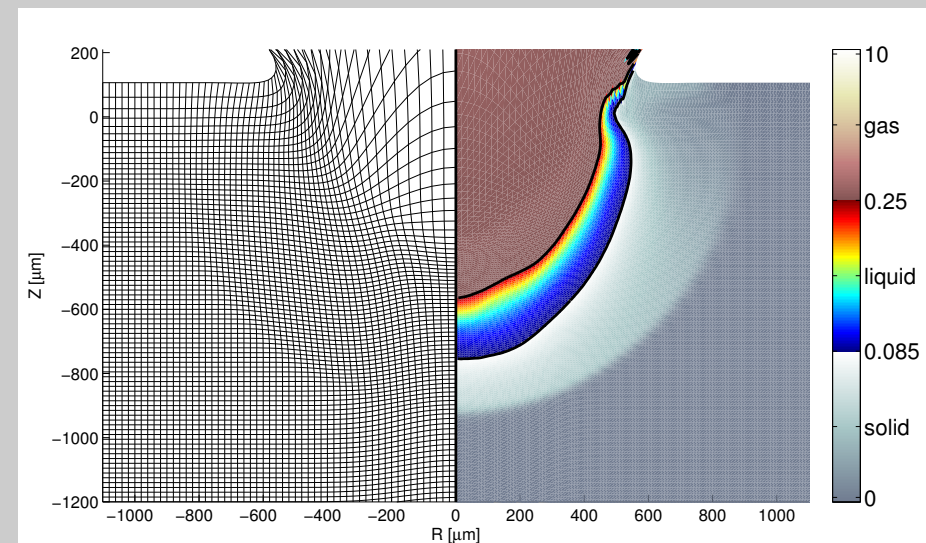
- Comparison of Lagrangian and ALE simulation short after computation starts, Lagrangian fails.
- ALE does not influence the result too much (slight shock diffusion), but mesh improved significantly.
- Impossible to finish simulation without ALE.

Laser examples: Disc impact – 3) impact, crater

- After impact – material compression, increase of temperature.
- Inside target: circular shock wave spreading from impact, melting and evaporation of target.
- Corona (plasma plume) spreading outside.

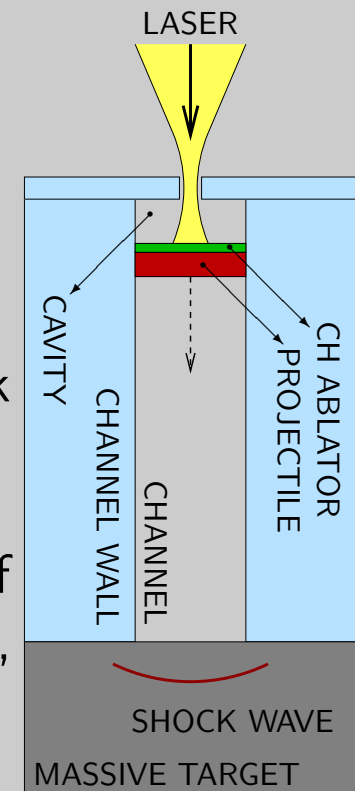
Laser examples: Disc impact – 3) impact, crater

- Crater formation – liquid/gas phase interface.
- Mesh remains smooth, the simulation can continue further.
- Comparison of craters sizes to experimental values – reasonable agreement^[1]



Laser examples: LICPA scheme

- Laser induced cavity pressure acceleration^[1].
- Preparation, analysis, interpretation of PALS experiments.
- Simulations of processes in channel covered by a cavity.
- Cavity \Rightarrow large portion of laser energy transferred to shock wave \Rightarrow higher impact velocity, larger craters.
- Many configurations: with of ablator/projectile, material of projectile/target (CH, Al, Cu, Au), laser energy (100 – 400 J), laser frequency (1ω , 3ω).
- Different aspects of experiments, hydroefficiency.
- Comparison of simulations and experiments (impact velocity, shock speed, crater size) \Rightarrow reasonably good agreement.



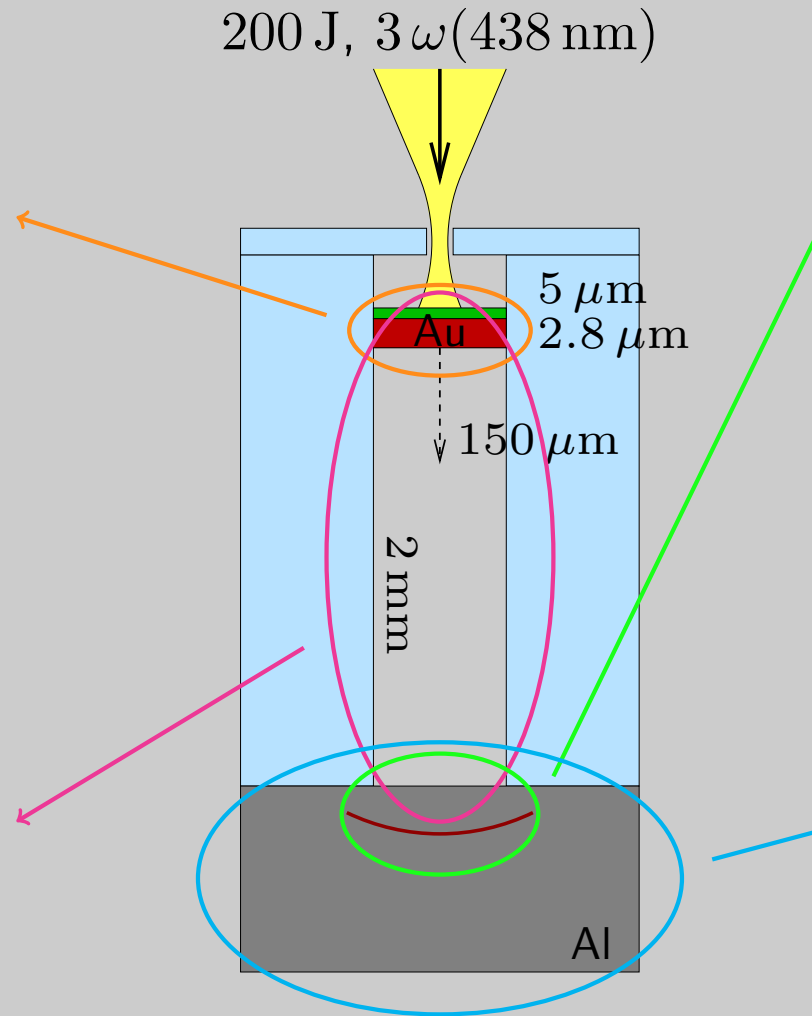
Laser examples: LICPA scheme

Absorption

Shock formation

Accel. + impact

Crater development



New trends in ALE hydrodynamics

- ALE+AMR (Adaptive Mesh Refinement)^[1]
 - automatically finer mesh in interesting regions (shocks, interfaces, physical phenomena, . . .);
 - higher effective resolution, uncomputable in whole domain;
 - necessary in Eulerian codes, useful in ALE.
- ReALE – reconnection ALE^[2]
 - changing mesh topology, cell follows the fluid;
 - significant improvement in regions of shear flows or vortices.
- Curvilinear ALE^[3] – curved mesh instead of straight
 - cell can significantly deform during fluid motion;
 - prevents most of tangling, increased robustness, less ALE.

[1] Anderson, Elliott, Pember: JCP, 2004.

[2] Loubere, Maire, Shashkov, Breil, Galera: JCP, 2010.

[3] Anderson, Dobrev, Kolev, Rieben, Tomov: SIAM JSC, 2018.

Conclusions

- Lagrangian and ALE methods suitable for laser/target simulations.
- Physical models crucial for realistic results.
- Current codes able to perform realistic laser/target computations.
- Ongoing research, attractive topic.

Thank you for your attention.